Journal of Textiles and Polymers

Vol. 12, No. 1, 27-34, March 2024
https://www.itast.ir
DOI: 10.48302/jtp.2025.542898.1319

Role of Geogrid's Structure on the California Bearing Ratio of the Reinforced Soil

Azita Asayesh[1*], Morteza Shahmohammadi[1], S. Majdeddin Mir Mohammad Hosseini[2]

[1] Textile Engineering Department, Amirkabir University of Technology, Tehran, Iran.
[2] Civil and Environmental Engineering Department, Amirkabir University of Technology,Tehran, Iran.

Article Information

Article history:

Received: 2025-08-23

Accepted: 2025-10-11

***Keywords*:**

Geogrid, warp knitted, California Bearing Ratio (CBR), fabric structure, tensile.

Abstract

The use of geosynthetic materials is a well-established and effective approach for reinforcing soil and improving its bearing capacity in geotechnical applications. Among these materials, geogrids have gained particular importance due to their ability to interlock with soil particles and enhance load distribution. In the present study, the effect of geogrid's structure on the California Bearing Ratio (CBR) of the reinforced soil has been investigated. For this purpose, warp-knitted polyester geogrids with various structures (Chain stitch + inlay, Tricot + inlay longitudinal ribs connected by inlay/weft yarns) were produced, coated, and tested for tensile strength and CBR. Results showed that geogrid reinforcement enhances soil CBR up to 20%, with a linear relationship between CBR and the ratio of geogrid elastic moduli in orthogonal directions. The geogrid structure significantly affected CBR, with Chain stitch/weft yarn configurations demonstrating superior reinforcement due to higher tensile strength and elastic modulus in both directions. The findings emphasize the significance of geogrid structure in enhancing soil reinforcement.

1 INTRODUCTION

Building pavements on weak soils is difficult. Highly compressible clay often shortens pavement lifespan. Geosynthetics are increasingly used to improve weak subgrade bearing capacity and reduce settlement. A key benefit is their ability to manage shear stresses from traffic at the base/subgrade interface. Their elastoplastic nature means they quickly stiffen under load, fully utilizing their tensile strength. Essentially, geosynthetics in reinforced soil bear the load, preventing excessive deformation. They achieve this by resisting tensile deformation and preventing soil slippage through bonding, adhesion, interlocking, and confinement, thus maintaining overall soil stability [1-2].

Extensive research has demonstrated the benefits of using geogrids and geotextiles to reinforce soil [3-12]. Mittal and Shukla [13] studied how biaxial geogrids improved the strength of weak subgrade soil. They found that embedding bitumen-coated geogrids in single or double layers at different depths improved the California Bearing Ratio (CBR) by up to 36% and 41%, respectively. Microscopic analysis confirmed that interlocking and friction between the soil and the geogrid fibers strengthened the soil. They also examined the combined effect of geotextiles and geogrids, which led to a higher maximum dry density than using geotextiles alone. The optimum moisture content differed as well. The combined reinforcement resulted in a higher CBR improvement (58%) compared to geotextile reinforcement alone (43%) [14]. Further investigation showed that the geotextile's confinement and the geogrid's interlocking effect increased the maximum dry density of reinforced soil samples compared to unreinforced soil. Maximum 40% and 60% CBR increments were achieved with double and triple-layer reinforcement, respectively [15-16].

Venkatesh and Suluguru [17] investigated the CBR of soil reinforced with geocells, geogrids, and geotextiles at different heights within the CBR mold (1/3H, 1/2H, 2/3H). All reinforced soils showed improved CBR values compared to unreinforced soil, with reinforcement being most effective at 1/3H from the top. Geocells provided the most remarkable CBR improvement compared to other geosynthetics. Among uniaxial, biaxial, and triaxial geogrids, the triaxial geogrid was most effective in increasing CBR values.

Shams et al. [18] examined the impact of geotextile placement on the CBR of clayey sandy soil reinforced with a single layer of nonwoven geotextile. They tested different geotextile depths within the mold. The presence of the geotextile layer increased the soil's load-bearing capacity. The optimal geotextile position was about 3.9 cm below the

* Corresponding author: a_asayesh@aut.ac.ir

surface, resulting in a CBR increase of up to 42.2% compared to unreinforced soil.

Ramjiram Thakur et al. [2] assessed the CBR improvement of clayey soil by reinforcing it with nonwoven geotextiles. They used thermally bonded nonwoven geotextiles (NW) and superior needle-punched nonwoven geotextiles (SNW) of varying thicknesses. The results indicated that reinforcing the soil with NW and SNW geotextiles increased its load-carrying capacity and reduced immediate settlement. Additionally, using thicker geotextiles led to higher CBR values.

Kumar and Rajkumar [19] found that incorporating woven and nonwoven geotextiles in unpaved roads, especially those with soft subgrades, improved penetration resistance and CBR strength. The performance of the unpaved road also improved at greater depths of penetration.

Lakshmi and Lakshmi [20] studied the effect of using woven (WG) and non-woven (NWG) geotextiles in reinforcing subgrade soil and enhancing its strength. Two types of coarse-grained soils with varying fine content were used. Geotextiles were placed at different depths (H/5, 2H/5, 3H/5, and 4H/5) to determine the impact on soaked and unsoaked California Bearing Ratio (CBR) strength. The ideal geotextile placement depth varied depending on the soil type and fine content. Soil reinforced with WG showed more significant strength gains than soil reinforced with NWG.

Baadiga and Balunaini [21] investigated the effect of geogrids in stabilizing soft subgrades using locally available soil. Large-scale lab experiments were conducted on subgrades with varying CBR values (2%, 5%, and 7%) overlaid with soil stabilized by polypropylene (PP) and polyethylene terephthalate (PET) geogrids. The study measured the modulus improvement factor (MIF) and improved CBR values. Results showed that geogrids, especially those with high stiffness, significantly improved subgrade CBR, with MIF values ranging from 1.2 to 2.8. The improvement was more significant for lower CBR subgrades and higher stiffness geogrids. A cost-benefit analysis indicated a potential cost reduction of about 48% using PP30 geogrid stabilization compared to cement stabilization.

In research by Poorahong et al. [22], the performance of pavement structures on soft clay subgrades reinforced with triaxial geogrids under static loading was surveyed. A large-scale test was conducted on pavement models with a crushed rock base and a soft clay subgrade, both with and without geogrid reinforcement. The geogrids were placed at the interface between the subgrade and base layers and at the mid-depth of the crushed rock base. Plate load tests revealed that two layers of geogrid reinforcement significantly improved the pavement's bearing capacity, with an improvement factor of 1.63 compared to the unreinforced pavement. This improvement was attributed to the geogrids changing the failure mode from punching and local shear failure to only punching failure.

Previous studies have primarily investigated the use of geogrids and geotextiles to enhance soil strength, particularly in terms of the California Bearing Ratio. However, no attention has been given to the influence of geosynthetic structural design on their reinforcing performance in soil. Since the structure of a material fundamentally determines its properties and functional behavior, this study addresses this gap by examining how fabric structure in textile-based geogrids affects both their tensile strength and their soil reinforcement efficiency.

2 MATERIALS AND METHODS

2-1 Materials

2-1-1 Soil

The soil used in this study is silica sand with rough and angular grains. The particle size distribution of the aggregates was determined according to ASTM C136-01[23], and the particle size distribution curve of the soil is illustrated in Fig.1.

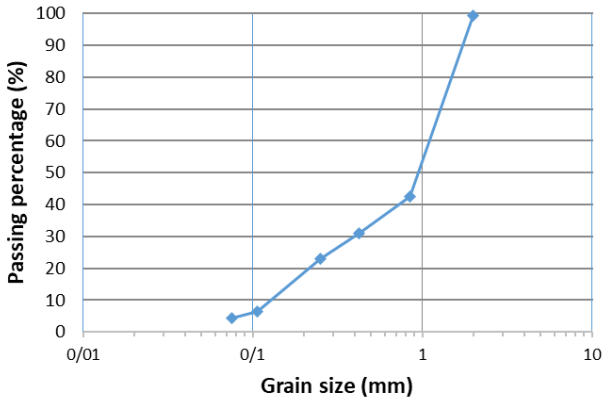

Fig. 1 The soil particle size distribution curve

2-1-2 Reinforcement

In this research, warp-knitted geogrids with five different structures were produced using polyester yarns (Table I) on a four-guide bars Raschel warp-knitting machine (model: Karl Mayer, Id: 51547, Gauge (NPI) 12) (Fig. 2). The lapping diagram and threading pattern of the guide bars for each geogrid structure are demonstrated in Table II. In the first three samples, the longitudinal ribs of the geogrids were knitted using Chain stitch and laid-in pattern. In contrast, the structure of the longitudinal ribs of the last two geogrids was a combination of Tricot and inlay yarn. The transverse connection of the longitudinal ribs was achieved using inlay yarn with a special pattern illustrated in Table II, except for the third and fifth samples (G3 and G5), in which the longitudinal ribs are connected by weft yarns inserted manually into the geogrid structure during the knitting process. High-tenacity polyester filament yarn with a count of 110 tex was utilized in manufacturing geogrid samples, except for Chain stitch and Tricot structures, which were knitted using 50 tex (16.7/3) polyester filament yarn. After knitting, the produced geogrids were coated with acrylic resin RSS-610.

Table 1 The characteristics of the yarns

Yarn type	Yarn count (tex)	Tensile strength (cN/tex)	Tensile strain (%)	Elastic modulus (cN/tex)
Polyester filament	16.7	34.25	23.07	300
High-tenacity polyester filament	110	65.76	10.13	727

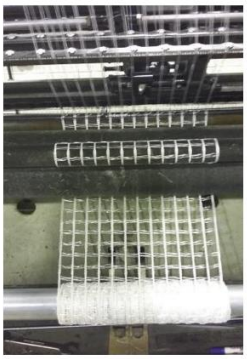

Fig. 2 The warp-knitting machine used to produce geogrids

The solution was subjected to 30 minutes of sonication. Following this, PCL was introduced into the ZnO and ZnO-Ag solutions, and the resulting mixtures were stirred for 12 h to create PCL-ZnO and PCL-ZnO-Ag blends. Notably, the blend solutions exhibited a homogeneous, colorless, and transparent appearance, with no signs of phase separation or precipitation observed. Table 1 provides a summary of the composition of the samples.

Table 2 Composition of samples

Sample No.	Nanofiber Sample	PCL (wt.%)	ZnO (wt.%)	Ag (wt.%)
1	PCL	15	0	0
2	PCL-ZnO	15	1	0
3	PCL-ZnO-Ag	15	1	0.5

Table 3 The structure of the produced geogrids

Sample code	Knitting lapping diagram		Threading pattern of the guide bars
G1	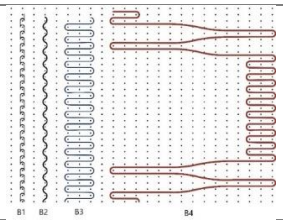	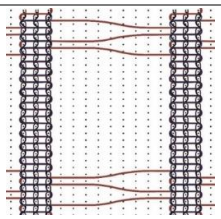	
G2	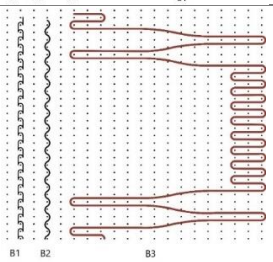	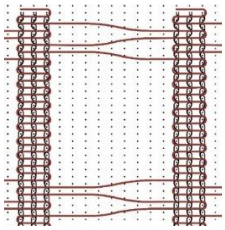	
G3	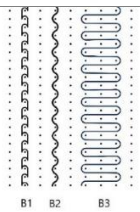	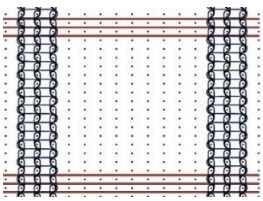	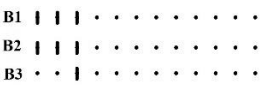
G4	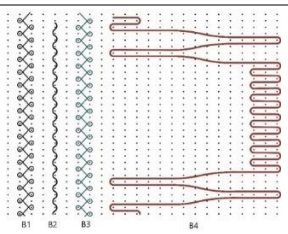	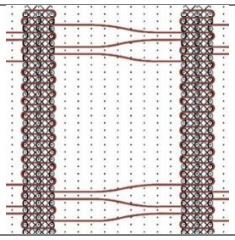	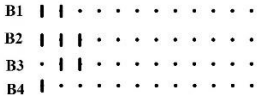
G5	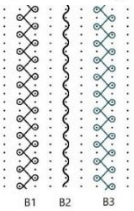	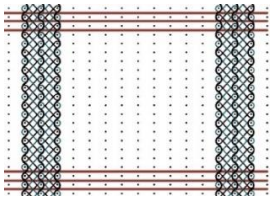	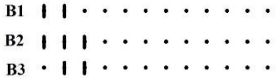

2-2 Physical properties measurement

2-2-1 Areal density

The areal density of each geogrid structure was measured according to ASTM D5261-10 [24], by weighing five samples with a size 15×15 cm2. The average results are presented in Table III.

2-2-2 Thickness

The thickness of geogrids was measured based on ASTM D5199-12 [25] using the Shirley digital thickness tester. The thickness of geogrids at the ribs' junctions has been evaluated under the pressure of 20g/cm2. The average results of ten measurements are presented in Table III.

2-3 Uniaxial tensile test

To determine the tensile properties of each geogrid structure, five samples were tested in both longitudinal and transverse directions, using an INSTRON Tensile Tester (Model 5566) according to ASTM D6637-01 (Method A) [26]. The test speed was 30 mm/min, and the distance between the device clamps was set to 4.5 cm to ensure that the two openings of the geogrid were placed between the clamps following the standard.

2-4 CBR test

To obtain the optimum soil moisture content for the CBR test, the laboratory compaction method according to ASTM D698-00A (Method A) [27] was used to determine the relationship between the water content and dry unit weight of the soil. To this end, the soil at a selected water content was placed in three layers into a mold of 101.6 mm diameter, with each layer compacted by 25 blows of a 24.4-N hammer dropped from a distance of 305mm. The resulting dry unit weight was determined. This procedure was repeated for the soil at five different moisture contents (7%, 10%, 13%, 16%, and %19%), and based on the relationship between the dry unit weight and the water content of the soil, the compaction curve of the soil was obtained. Eventually, values of the optimum water content and the maximum dry unit weight were determined from the compaction curve.

The CBR test was conducted using a CBR test machine (Fig. 3) based on ASTM D 1883 – 07 [28] at the optimum water content of the soil (12.2%), which was obtained through the compaction test previously. The soil was compacted at three densities (10, 25, and 56 blows). For each density, the soil was placed in three layers into a mold of 152.2 mm diameter, with each layer compacted by a related number of blows (10, 25, and 56) of a 24.4N hammer dropped from a distance of 305 mm. For reinforced soil, the geogrid was placed in the mold after the first layer of compaction of the soil. In other words, the geogrid was located 40 mm below the surface layer of the soil. Penetration testing was accomplished by the compression machine using a strain rate of 1.27 mm/min. According to the standard, reading of loads was taken at penetrations of 0.64 mm, 1.27 mm, 1.91 mm, 2.54 mm, 3.18 mm, 3.81 mm, 4.45 mm, 5.08 mm, 7.62 mm, 10.16 mm, and 12.70 mm.

a b

Fig. 3 CBR test: a) The CBR test machine, b) Geogrid placement in the mold

3 RESULTS AND DISCUSSIONS

3-1 Results of tensile test

The average tensile stress-strain curves of the produced geogrids in the longitudinal (wale-wise) and transverse (course-wise) directions are illustrated in Fig. 4, and their engineering properties are presented in Table III. For all geogrids, the aperture size and width of the ribs were 2×2 cm² and 0.5 cm, respectively.

Since the weights of geogrids are different, the stress-strain curves are normalized by the weight of the geogrids. The slope of the linear region in the normalized stress-strain curves was taken as the initial tensile modulus of the geogrids.

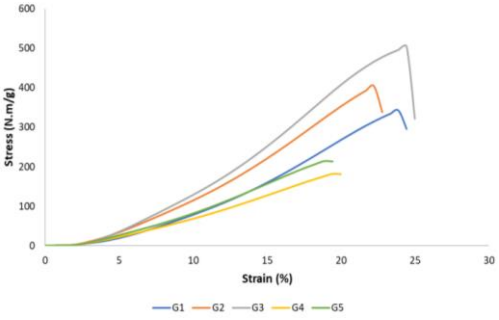

a

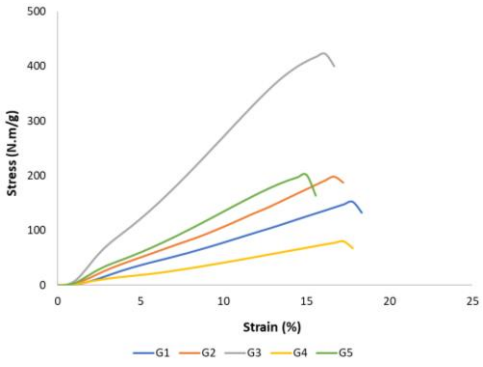

b

Fig. 4 Normalized tensile stress-strain curves of the geogrids, a) longitudinal direction, b) transverse direction

Table 4 The engineering properties of the geogrids

Geogrid code		G1	G2	G3	G4	G5
Thickness (mm)		1.46	1.31	1.26	1.83	1.86
Areal density(g/m^2)		149	127	113	272	230
Ultimate tensile strength (N.m/g)	Wale wise direction	342.5	403.2	504.1	181.6	214.4
	Course wise direction	152.7	198.5	422.8	79.6	201
Tensile strain at failure (%)	Wale wise direction	23.8	22.2	24.4	19.4	19
	Course wise direction	17.8	16.7	16.1	17.2	15
Initial tensile modulus (N.m/g)	Wale wise direction	1121.5	1371.6	1610.6	587.5	715.2
	Course wise direction	1048.8	1238.8	3502.5	550	1268.8

As seen in Fig. 5a and Table III, the geogrids whose longitudinal ribs are knitted with Chain stitch (G1 to G3) exhibit higher tensile strength and elastic modulus in the longitudinal (wale) direction than those knitted with Tricot structure (G4 and G5). This can be attributed to the fact that, in Chain stitch structure (Table I), the underlaps of the loops are zero, and the loops are formed in the loading direction. Consequently, the fabric resists deformation when subjected to the load. In contrast, in the Tricot structure (Table I), due to deviation of the underlaps from the loading direction, the fabric's resistance to deformation is less than Chain stitch structure.

Furthermore, Fig. 5b and Table III reveal that the geogrids whose longitudinal ribs are connected by weft yarns (G3 and G5) demonstrate higher tensile strength and elastic modulus in the transverse direction (course) than those connected with inlay yarns (G1, G2, and G4). Of course, this finding is more pronounced in the case of sample G3, with a Chain stitch structure in its longitudinal ribs. The reason is that in weft-inserted structures, the weft yarns are straight in the geogrid structure and lie in the loading direction. In contrast, in laid-in structures, the inlay yarns are not entirely straight and, to some extent, deviate from the loading direction. Therefore, geogrids consisting of weft yarns resist deformation more when subjected to the load in the course direction.

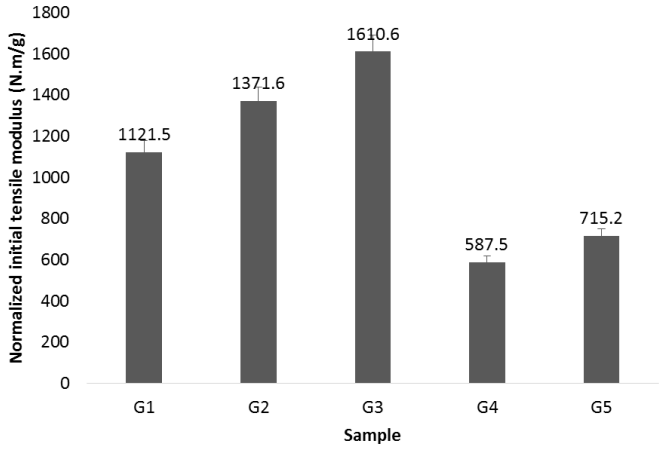

a

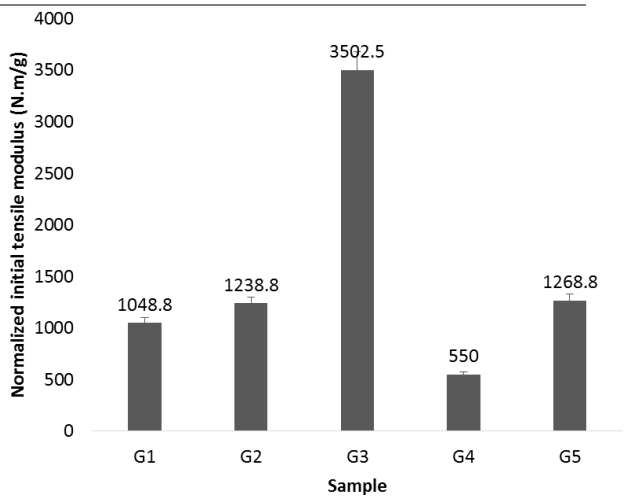

b

Fig. 5 The normalized initial tensile modulus of the geogrids, a) longitudinal direction, b) transverse direction

3-2 Results of CBR test

During the CBR test, the load values for different penetrations were recorded. By calculating the penetration stress in kPa, the curve of penetration resistance (stress) vs. penetration was plotted for each sample. A typical penetration resistance vs. penetration graph for reinforced soil compacted at different densities is shown in Fig. 6. Also, the graphs of stress-penetration for unreinforced soil and reinforced soil with various geogrids are illustrated in Fig. 7, for the soil compacted with 25 blows. At the onset of the loading, there is a high resistance to penetration; thereafter, the penetration rate continues to increase, but at a steady state. These figures reveal that increasing soil compaction improves soil resistance to penetration. Moreover, the reinforced soil resists penetration more than the unreinforced soil, and this resistance is more pronounced in soils reinforced with geogrids whose longitudinal ribs are connected by weft yarns.

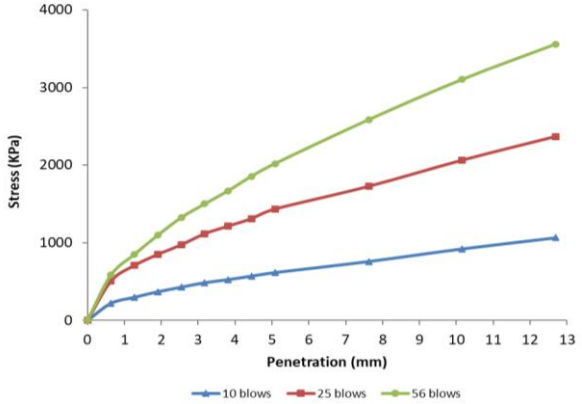

Fig. 6 Stress-penetration curves for reinforced soil with geogrid G3

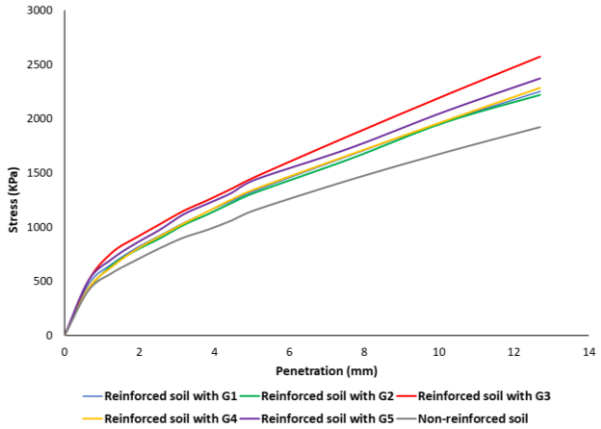

Fig. 7 Stress-penetration curves for unreinforced and reinforced soils with various geogrids

To achieve the CBR values, for each sample the penetration resistance for 2.5 mm and 5 mm were obtained from the stress-penetration curve, and the corresponding CBR was calculated by dividing the penetration stresses by the standard stress of 1000 psi (6900 kPa) and 1500 psi (10,300 kPa), respectively and multiplying by 100 (Equation 1). The desired CBR value was chosen as the greater of the computed values at 2.5 mm and 5 mm penetration.

$$\text{CBR} = \frac{\text{Stress (kPa)}}{\text{Standard Stress (kPa)}} \times 100 \quad (1)$$

After calculating the CBR values for each sample at three different soil densities, the curves of CBR vs. dry density of the soil were plotted (Fig. 8), and CBR values for each sample were obtained at 1.917 g/cm3, which is the soil dry density at optimum moisture content. The achieved CBR values for unreinforced and reinforced soils with geogrids are presented in Table IV.

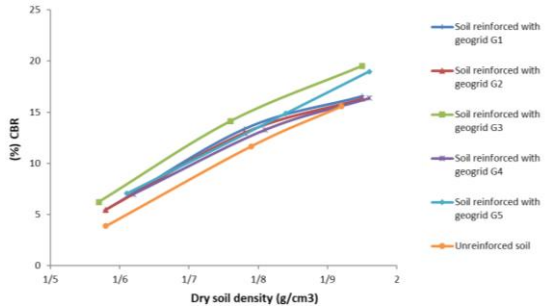

Fig. 8 The CBR vs. dry density of reinforced and unreinforced soils with various geogrids

Table 5 CBR test results for unreinforced and reinforced soils with various geogrids

Soil condition	CBR (%)	Increase in CBR (%)
Unreinforced	15.47	-
Reinforced with geogrid G1	16.02	3.56
Reinforced with geogrid G2	15.73	1.68
Reinforced with geogrid G3	18.62	20.36
Reinforced with geogrid G4	15.57	0.64
Reinforced with geogrid G5	17.5	13.12

It can be seen that reinforcing the soil with geogrid increases the CBR of the soil, and the increment is higher for soil reinforced with geogrids whose longitudinal ribs are connected by weft yarns than that of inlay yarn. Furthermore, among the weft-inserted geogrids, the one whose longitudinal rib is knitted by Chain stitch enhances the CBR of the soil more than that with Tricot structure.

The mobilization of soil strength via reinforcing geosynthetic material is based on the general lateral restraints caused by the frictional interaction and interlocking between soil particles and geosynthetics. Owing to the good interlocking and frictional capabilities of the utilized geogrids, they provide tensile resistance to any further lateral movements and therefore improve the strength of the soil [29-30]. Consequently, they help improve the bearing capacity of the soil by forcing the potential bearing capacity failure surface to move to an alternate, higher-strength path.

Another reason for the improvement in the strength of the soil is that during the CBR test, plastic deformation occurs in the weak soil, leading to higher friction between the geogrid and soil particles. In the reinforced soil, the tensile stresses develop in the geogrid membrane, and due to the high tensile modulus of the geogrid, it can help the weak soil to support the applied stress due to loading. A geogrid with a higher modulus would provide more support to the soil, and strengthening of the soil would be more effective. As mentioned previously, among the considered geogrid structures, sample G3 possesses the highest initial modulus in both wale and course directions. Therefore, it is expected that geogrid G3 with Chain stitch structure and connection of the ribs by weft yarns provides the highest reinforcement for the soil, which is expected as can be seen in Table IV.

The relation between the CBR of the soil and the elastic modulus of the geogrids in the orthogonal directions is illustrated in Fig. 9. As seen, there is a linear relation with a high correlation coefficient (R^2= 0.98) between the CBR of the soil and the ratio of elastic modulus of the geogrids in the transverse direction (E_T) to that of the longitudinal direction

(E_L). It can be concluded that according to equation (2), the CBR of the reinforced soil increases as the ratio of elastic modulus of the geogrids in the orthogonal directions increases.

$$CBR(\%) = 2.2138 \left(\frac{E_T}{E_L}\right) + 13.711 \quad (2)$$

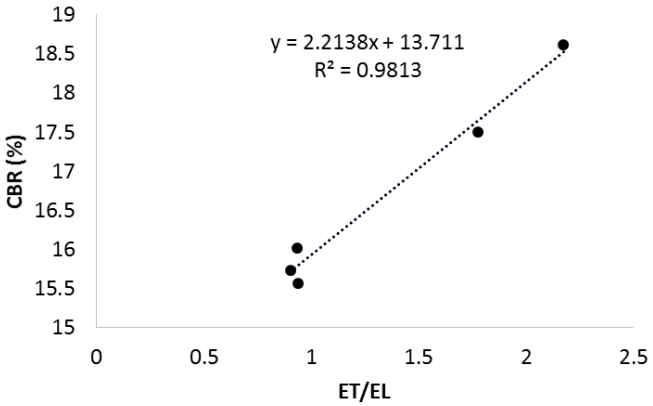

Fig. 9 Correlation between CBR and elastic modulus of the geogrids

4 CONCLUSIONS

This study decisively identified the optimal structural design for enhanced soil reinforcement using warp-knitted polyester geogrids. The principal outcomes demonstrated clear performance differences based on rib construction. Geogrids utilizing the Chain stitch pattern in their lengthwise ribs exhibited notably greater strength and stiffness along the longitudinal direction compared to those made with a Tricot structure. The strategic replacement of inlay yarns with weft yarns for connecting the lengthwise ribs significantly improved the geogrid's strength and stiffness in the transverse (crosswise) direction. Overall, the application of these geogrids resulted in a measurable improvement in the soil's California Bearing Ratio (CBR). A key finding established a direct, positive relationship between the resulting soil CBR and the geogrids' elastic modulus in both the lengthwise and crosswise directions. The design combining the Chain stitch lengthwise ribs and weft yarns crosswise provided the best soil reinforcement results. This specific geogrid achieved superior performance because it delivered the highest overall strength and elastic modulus across both primary axes.

REFERENCES

[1] Rajesh, U., Sajja, S., Chakravarthi, V.K., 2016. Studies on the engineering performance of geogrid-reinforced soft subgrade, Transportation Research Procedia, 17, pp.164-173

[2] Ramjiram Thakur, S., Naveen, B.P., Tegar, J.P., 2021. Improvement in CBR value of soil reinforced with nonwoven geotextile sheets, International Journal of Geo-Engineering, 12(1), pp.1-10

[3] Rudramurthy, M., Vikram, M.B., 2016. Effect of geotextiles on CBR values, International Journal of Emerging Trends in Engineering and Development, 1(6), pp.118-125

[4] Naeini, S.A., Mirzakhanlari, M., 2008. The effect of geotextile and grading on the bearing ratio of granular soils, EJGE, 13, pp.1-10

[5] Kumar, P.S., Devi, S.P., 2011. Effect of needle punched nonwoven coir and jute geotextiles on CBR strength of soft subgrade, ARPN Journal of Engineering and Applied Sciences, 6, pp.114-116

[6] Ogundare, D.A., Familusi, A.O., Osunkunle, A.B., Olusami, J.O., 2018. Utilization of geotextile for soil stabilization, American Journal of Engineering Research (AJER), 7(8), pp.224-231

[7] Hossain, A., Adnan, A., Alam, M.M., 2015. Improvement of granular subgrade soil by using geotextile and jute fiber, International Journal of Science, Technology and Society, 3(5), pp.230-235

[8] Singh, P., Gill, K.S., 2012. CBR improvement of clayey soil with geogrid reinforcement, International Journal of Emerging Technology and Advanced Engineering, 2(6), pp.456-462

[9] Adams, C.A., Apraku, E., Opoku-Boahen, R., 2015. Effect of triaxial geogrid reinforcement on CBR strength of natural gravel soil for road pavements, Journal of Civil Engineering Research, 5(2), pp.45-51

[10] Kuity, A., Roy, T.K., 2013. Utilization of geogrid mesh for improving the soft subgrade layer with waste material mix compositions, Procedia-Social and Behavioral Sciences, 104, pp.255-263

[11] Duncan-Williams, E., Attoh-Okine, N.O., 2008. Effect of geogrid in granular base strength–An experimental investigation, Construction and building materials, 22(11), pp.2180-2184

[12] Adams, C.A., Tuffour, Y.A., Kwofie, S., 2016. Effects of soil properties and geogrid placement on CBR enhancement of lateritic soil for road pavement layers, American Journal of Civil Engineering and Architecture, 4(2), pp.62-66

[13] Mittal, A., Shukla, S., 2019. Strength improvement of poor subgrade soil reinforced with polyester biaxial geogrid, Jordan Journal of Civil Engineering, 13(2), pp.214-225

[14] Mittal, A., Shukla, S., 2018. Influence of geotextile and geogrid reinforcement on strength behaviour of soft silty soil, Applied Mechanics and Materials, 877, pp.264-269

[15] Mittal, A., Shukla, S., 219. Effect of geosynthetic reinforcement on strength behaviour of weak subgrade soil, Materials Science Forum, 969, pp.225-230

[16] Mittal, A., 2018. Effect of non-woven geotextile and biaxial geogrid reinforcement on the strength behaviour of subgrade soil, International Journal of Civil Engineering, 5(10), pp.28-32

[17] Venkatesh, G., Suluguru, A.K., 2020. Effective study of geocell, geogrid and geotextile as geo-reinforcement on CBR and resilient modulus value of subgrade, Solid State Technology, 63, pp.2557-2573

[18] Shams, B., Ardakani, A., Roustaei, M., 2020. Laboratory investigation of geotextile position on CBR of clayey sand soil under freeze-thaw cycle, Scientia Iranica, 27(6), pp.2808-2816

[19] Kumar, P.S., Rajkumar, R., 2012. Effect of geotextile on CBR strength of unpaved road with soft subgrade, Electronic Journal of Geotechnical Engineering, 17(1), pp.1355-1363

[20] Lakshmi, S.M., Lakshmi, S.V., 2023. Soil strength improvement by reinforcing soil with geotextiles. Materials Today: Proceedings, 22

[21] Baadiga, R., Balunaini, U., 2024. Effective CBR and Elastic Modulus of Geogrid-Stabilized Prepared Subgrades Overlying Existing Soft Subgrades, International Journal of Geosynthetics and Ground Engineering, 10(41), pp.1-17

[22] Poorahong, H., Jamsawang, P., Thanasisathit, N., Jongpradist, P., Jing, G., 2024. Performance of a triaxial geogrid-reinforced crushed rock base underlain by a soft clay subgrade, Case Studies in Construction Materials, 20, p.e03198.

[23] ASTM C136-01. (2020) Standard Test Method for Sieve Analysis of Fine and Coarse Aggregates.

[24] ASTM D5261-10. (2018) Standard Test Method for Measuring Mass per Unit Area of Geotextiles.

[25] ASTM D5199-12. (2019) Standard Test Method for Measuring the Nominal Thickness of Geosynthetics.

[26] ASTM D6637-01 (2010) Standard Test Method for Determining Tensile Properties of Geogrids by the Single or Multi-Rib Tensile Method.

[27] ASTM D698-00A. (2021) Standard Test Methods for Laboratory Compaction Characteristics of Soil Using Standard Effort.

[28] ASTM D 1883 – 07 (2010). Standard Test Method for CBR (California Bearing Ratio) of Laboratory-Compacted Soils.

[29] Perkins, S.W., Ismeik, M. A., 1997. Synthesis and evaluation of geosynthetic-reinforced base layers in flexible pavements-part i., Geosynthetics International, 4(6), pp.549-604

[30] Tutumluer, E., Kang, M., Qamhia, I.I., 2025. Geosynthetic stabilization of road pavements, railroads, and airfields, Transportation Geotechnics, 50, p.101321.